Article

Atmospheric Reactivity of Fullerene (C$_{60}$) Aerosols

Dhruv Mitroo,[†,‡] Jiewei Wu,[†] Peter F. Colletti,[†] Seung Soo Lee,[†] Michael J. Walker,[†] William H. Brune,[§] Brent J. Williams,*,[†] and John D. Fortner*,[†]

[†]Department of Energy, Environmental and Chemical Engineering, Washington University in St. Louis, St. Louis, Missouri 63130, United States

[§]Department of Meteorology and Atmospheric Sciences, The Pennsylvania State University, University Park, Pennsylvania 16802, United States

S Supporting Information
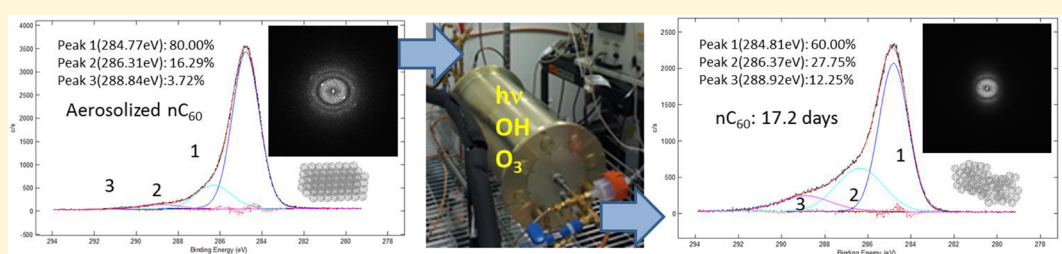
ABSTRACT: Rapid growth and adoption of nanomaterial-based technologies underpin a risk for unaccounted material release to the environment. Carbon-based materials, in particular fullerenes, have been widely proposed for a variety of applications. A quantitative understanding of how they behave is critical for accurate environmental impact assessment. While their aqueous phase reactivity, fate, and transport have been studied for over a decade, aerosol phase reactivity remains unexplored. Here, the transformation of C$_{60}$, as nanocrystal (nC$_{60}$) aerosols, is evaluated over a range of simulated atmospheric conditions. Upon exposure to UV light, gas-phase O$_3$, and $^\bullet$OH, nC$_{60}$ is readily oxidized. This reaction pathway is likely limited by diffusion of oxidants within/through the nC$_{60}$ aerosol. Further, gas-phase oxidation induces disorder in the crystal structure without affecting aerosol (aggregate) size. Loss of crystallinity suggests aged nC$_{60}$ aerosols will be less effective ice nuclei, but an increase in surface oxidation will improve their cloud condensation nuclei ability.

KEYWORDS: fullerenes, nC$_{60}$, nanocrystals, oxidation, potential aerosol mass (PAM) reactor, atmospheric aging

INTRODUCTION

Industrial scale production and adoption of engineered nanomaterials raise concerns over their inadvertent impacts on human health and natural systems.[1,2] Of these, carbon based nanoscale materials such as fullerenes, carbon nanotubes (CNTs), and graphene are being developed for a variety of applications.[3−5] Fundamental understanding of how such materials behave when released in fluvial, marine, or atmospheric systems is critical for material design, life cycle analyses, risk assessment, and eventual effective waste management. In contrast to aqueous systems, atmospheric aerosol release scenarios have only recently been considered for engineered nanomaterials, such as carbon nanotubes (CNTs) and fullerenes, and inorganic nanoparticles, such as TiO$_2$.[2,6,7] In particular, the fate of fullerenes in aqueous systems is being studied extensively.[8−10] In the atmosphere, fullerenes have been identified in sooty flames[11] and lightning:[12] high energy (and high temperature) processes. To date, there is little understanding of how low-energy events (relative to formation events), such as atmospheric processing (e.g., photo-oxidation)[13] of fullerenes may alter their physicochemical properties and, thus, their behavior, which is a critical knowledge gap for

accurate modeling of solubility, (bio)availability, reactivity, stability, and toxicity.

In the aqueous phase, C$_{60}$ (as nC$_{60}$) is readily oxidized in absence of light with both ozone, yielding hemiketal and hydroxyl functionalities proposed via a modified Criegee mechanism, and by hydroxyl radicals, forming hydroxylated fullerenes.[8,14] Recently, Wu et al. found that free chlorine also oxidizes nC$_{60}$ in aqueous media, eventually altering the nanoparticles' crystal structure.[15] Because the cage structure imposes strain on its aromatic rings, epoxide formation is unstable, and water hydrolyzes intermediate structures to yield C=O or C−OH functional groups.[16−18] Further, UV light has been shown to sensitize aqueous phase reactions leading to oxidation products including epoxides and ethers.[19] Previously, Foote et al. proposed an energy transfer mechanism whereby photons excite ^{1}C$_{60}$ to an excited state, ^{1}C$_{60}$*, leading through intersystem crossing (ISC) to the triplet excited state ^{3}C$_{60}$*.[20] Then, through a type II energy transfer mechanism, this can

convert excited triplet oxygen $^3O_2$ to singlet oxygen, $^1O_2$.[20] Krusic et al. instead proposed a type I mechanism where $^3C_{60}$* forms an anion in the presence of an electron donor.[21] Both pathways have been shown to generate reactive oxygen species (ROS).[22] The generation of the radical anion has been also observed in aqueous phase nC_{60} aggregates as well, also generating ROS.[23]

With regard to the atmosphere (troposphere), nC_{60} chemistry is largely unexplored. To date there are three reported field observations of airborne fullerenes (without distinguishing between their molecular and aggregated states),[24,25] one systematic laboratory study of atmospheric ozonolysis of fullerene,[26] and one of atmospheric ozonolysis/photooxidation of CNTs.[27] Wang et al. and Utsunomiya et al. observed fullerenes in carbonaceous aerosol samples in Nanjing, China and Detroit, Michigan, respectively.[24,28] Additionally, Sanchis et al. reported aerosol-bound fullerenes in samples collected in two campaigns covering different regions of the Mediterranean.[25] In addition to these campaigns, fullerenes have been identified in other airborne samples,[29] further highlighting the importance of understanding fullerene behavior and reactivity in the atmosphere. However, atmospheric processing of these fullerenes has not been investigated or discussed. Recently, Tiwari et al. explored atmospheric ozonolysis of C_{60} bulk fullerene powder through lab studies, demonstrated that atmospheric time scales can accommodate surface reaction of potential fullerene aerosols.[26] Similarly, Liu and co-workers investigated atmospheric photo-oxidation of CNTs via both ozone and hydroxyl attack, suggesting evidence of processing, and raising concern over gas-particle partitioning of organics in CNTs during atmospheric evolution.[27] In both studies, commercially available C_{60} powder and CNTs of fixed (commercial grade) purity and aggregate size were used. Other studies concerning aerosol-phase heterogeneous (gas-phase reaction on the surface of a solid particle) oxidation via ozone or hydroxyl radicals have investigated the chemistry of nonaromatics, such as oleic/stearic acid particles,[30] squalene,[31] palmitic acid,[32] and erythritol and levoglucosan;[33] aromatics including surface-bound polycyclic aromatic hydrocarbons (PAHs).[34−36] To date, to the best of our knowledge, none have looked at engineered nanoparticles.

Here, we present direct evidence of atmospherically relevant heterogeneous reactions of nC_{60} aerosols by simultaneous ozone and hydroxyl radical oxidation in the presence of UV light using a potential aerosol mass (PAM) reactor,[37] an oxidative flow-tube reactor (OFR). Atmospheric exposure, or mimicked "age", of the aerosol spans between ∼0−2 weeks, over which, we monitor physical and chemical changes to the nC_{60} aerosols. Surface oxidation, crystal structure, and aggregate (aerosol) size are described as a function of exposure in the gas-phase.

■ MATERIALS AND METHODS

Setup. For this study, nC_{60} was synthesized as described previously in detail by Fortner et al.[8] The experimental setup schematic for the aerosol-phase oxidation study is available in the Supporting Information (Figure S1), along with a description of the nC_{60} synthesis (section titled nC_{60} nanocrystal synthesis). Briefly, a 25 mg L^{-1} nC_{60} suspension was atomized in a 6-jet Collison Nebulizer (BGI, Inc.; Waltham, MA) and passed through an inlet heated to ∼100 °C to drive surface water off the aerosolized particles. Half of the flow (corresponding to 5.0 L min^{-1}) was sent to the PAM reactor

via a custom-built diffusion dryer to remove water vapor from the aerosol stream. Relative humidity (RH) control in the PAM chamber was achieved by adding 4.6 L min^{-1} of N_2 flow with fixed humidity. Additional details can be found in the Setup details section in the Supporting Information. Reported negative ζ-potential measurements of the nC_{60} aqueous suspensions,[38] suggesting that electrostatic repulsion is important in stabilizing the suspensions. If aggregation of primary nC_{60} nanoparticles does not occur in suspension, then drying should not induce further clustering. This was the case for our system (see Figure S2), where the mode of the size distribution in the aerosol phase was comparable to that of the aqueous phase.

Reactor. The custom built PAM reactor is an iridite-treated aluminum cylinder, 18 in. in length and 8 in. in inner diameter, giving it a total volume of 13 L. The chamber is equipped with two 12 in. mercury lamps with peak wavelengths at 185 and 254 nm (BHK Inc. Analamp Model No. 82−9304−03; Ontario, CA) housed in Teflon sheaths. There is an annular flow of N_2 through the sheaths to prevent direct contact with the lamps and purge any outgas products. The mercury lamps are connected to a variable voltage supply (BHK Inc.; Ontario, CA) to regulate light intensity. The former wavelength is necessary for the O_2 photolysis to produce O_3, and the latter dissociates O_3 to form singlet oxygen, $O(^1D)$, which in the presence of H_2O can form a hydroxyl radical.[37] Teflon sheaths are transparent to both wavelengths. Additional ozone is delivered to the inlet of the PAM to accelerate production of hydroxyl radicals. A simplistic mechanism of oxidant formation can be found in the Supporting Information, eqs 3−7 and more refined mechanisms are available in the literature.[39−43] At a fixed 10 L min^{-1} flow rate, the mean residence time for the nC_{60} aerosol in the reactor, τ_{res}, (defined by the volume of the reactor divided by the outlet flow rate) is approximately 78 s. This parameter is held constant throughout the study. Typically, heterogeneous reactions in OFRs conducted by other groups are performed at RH in the range of ∼10−60%.[40,41,44,45] For our study, RH was chosen at ∼30% (dry conditions to avoid potential deliquescence of aerosols, yet high enough to promote ●OH formation) and kept constant since the mixing ratio of water directly affects hydroxyl radical production (Supporting Information eq 7).[41]

OH Exposure. The reactor can generate hydroxyl radicals in mixing ratios >1000 ppt, which is several order-of-magnitudes higher than atmospheric concentrations (typically <1 ppt),[46] resulting in an exposure equivalent of over two weeks (ca. two weeks is an average aerosol lifetime[47]) in the atmosphere over a relatively short physical τ_{res}. At a fixed RH, hydroxyl radical generation can be controlled by varying the UV light intensity (please refer to Figure S3 for reactor calibration). Calculated OH exposure,[44] which is the product of [●OH] and τ_{res}, expressed in units of molec. cm^{-3} s, is then used to assess the "age" of the aerosol by comparing its value to an average tropospheric value. Renbaum and Smith studied the interchangeability of [●OH] and τ_{res} in flow-tube reactors, concluding that as long as reaction is limited to the surface (i.e., surface kinetics are much faster than bulk diffusion), then the simulated aging process in the reactor is atmospherically relevant.[45] Tiwari and co-workers suggested that, for ozonolysis of bulk C_{60} aerosol in their 6 m^3 PTFE chamber, reaction was likely limited to the surface.[26] In this manuscript, we provide evidence that mixed ozonolysis/photo-oxidation reaction is limited to the nC_{60} nanoparticle surface.

■ RESULTS AND DISCUSSION

C_{60} oxidation in the aqueous-phase can affect nanoparticle (nC_{60}) stability by forming (more) water-soluble products,[8] causing these nanoparticles to become smaller upon dissolution of outer layers. In this work, no appreciable change occurred in the aerosols' geometric mean mobility diameter (D_{Pg}) over the full range of exposure times (Figure 1) (details of the plot can
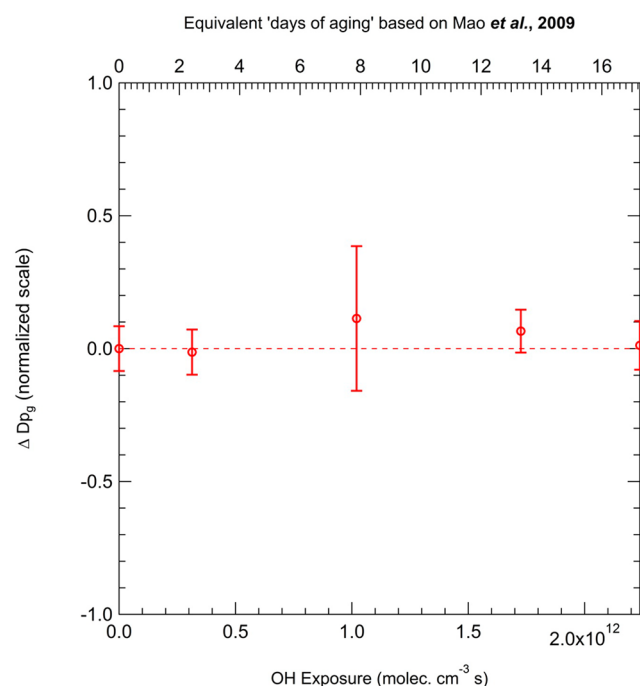

Figure 1. Change in the geometric mean mobility diameter (Dp_g) of aerosolized nC_{60} as a function of OH Exposure for mixed OH/O_3 oxidation. Values are normalized by an average Dp_g for unoxidized nC_{60} (control, see SI), and the bias associated with the control Dp_g is subtracted.

be found in the Supporting Information). Because the aerosolized nanoparticles did not change in size over simulated aging processes, either they did not react beyond the surface layer in a gas-phase oxidizing environment, or the product behavior is different from that in the solvent phase. On the basis of the exceedingly low vapor pressure of fullerenes/products (based on molecular weight), we do not expect to lose any material to the gas phase. Further, as observed for aqueous studies, oxidative chemical reactions should result in functionalization rather than fragmentation (e.g., C═C bond cleaving that is suggested for benzene[48] should be suppressed on account of stearic hindrance), as seen by Tiwari et al. as well as other aromatic and PAH oxidation pathways.[26,49,50] Oxygenated products, for example fullerol (a general term of hydroxylated fullerenes), can have dynamic physiochemical properties in solution, including significantly enhanced solubility and altered reactivity.[51] In an aqueous media, reacted molecules on the outer layer of the crystal can effectively "peel" off (dissolve) into the solution, leaving a hydrophobic core to be oxidized and subsequently dissolved. However, this process is not feasible in the gas phase, as there is no polar solvent phase for the oxidized layer to dissolve into. If surface saturation occurs, the only way for reaction to proceed is either diffusion of oxidants through the outer lattice, or self-reaction of outer layer products with the unreacted core. The

degree to which these interactions are relevant, or even rate limiting, may change for a deliquesced aerosol.

Surface Reactions. Fourier transform infrared spectroscopy (FTIR) data was obtained for samples at two different oxidation extents (Figure 2). Adsorption peaks at ~520 and
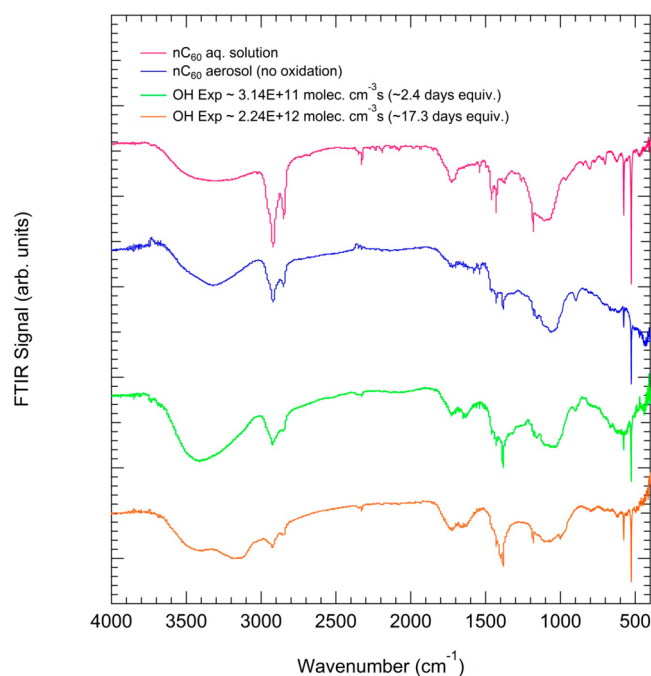
Figure 2. Offset FTIR spectra for nC_{60} samples collected on PTFE filters at different levels of OH Exposures for mixed OH/O_3 oxidation. Peaks around ~1400 and 1700 cm^{-1} indicate of C−OH and C═O groups, respectively.

570 cm^{-1} in the data, representative of C═C vibration modes from pristine nC_{60}, do not decrease appreciably during oxidation, suggesting incomplete conversion of the core material to a more oxidized product. However, peaks around 1400 and 1650 cm^{-1} (the latter appears to develop with age), indicative of C−OH and C═O groups, respectively,[8,19,52] are more pronounced at higher levels of oxidation. Despite not having the characteristic broad peak at 3000−3500 cm^{-1} characteristic of C − OH in plane bending (as found, for example, in fullerol, standards),[8] there is a clear peak development as a function of reaction time. The distinguishing peak in this range, which appears at the highest OH exposure, may not represent the C−OH in plane bending because of its narrow breadth around ~3200 cm^{-1}; however, it does overlay onto the double peak at ~2800 and 2900 cm^{-1}. In a recent study, Wu et al. observed the transformation of hydrogenated fullerenes (fulleranes) under different oxidizing environments. Fulleranes have very strong absorbance at ~2800 and 2900 cm^{-1} (double peak), which is lost upon oxidation.[53] It would be unlikely that reduced fulleranes are formed in our system from hydrolysis of OH-adducts on nC_{60}, hence we believe the double peaks are being overshadowed by an unknown evolution at ~3200 cm^{-1}, and their presence to begin with is due to the synthesis process. As reacted nC_{60} was not resuspended in a solvent for analysis (i.e., analytes were not extracted from filters by toluene[54−56] for FTIR analysis), exposure to further potential oxidants/ligand chemistry was avoided and thus chemical alterations were a direct result of processing in the PAM reactor. Surface oxidation analysis was done by X-ray
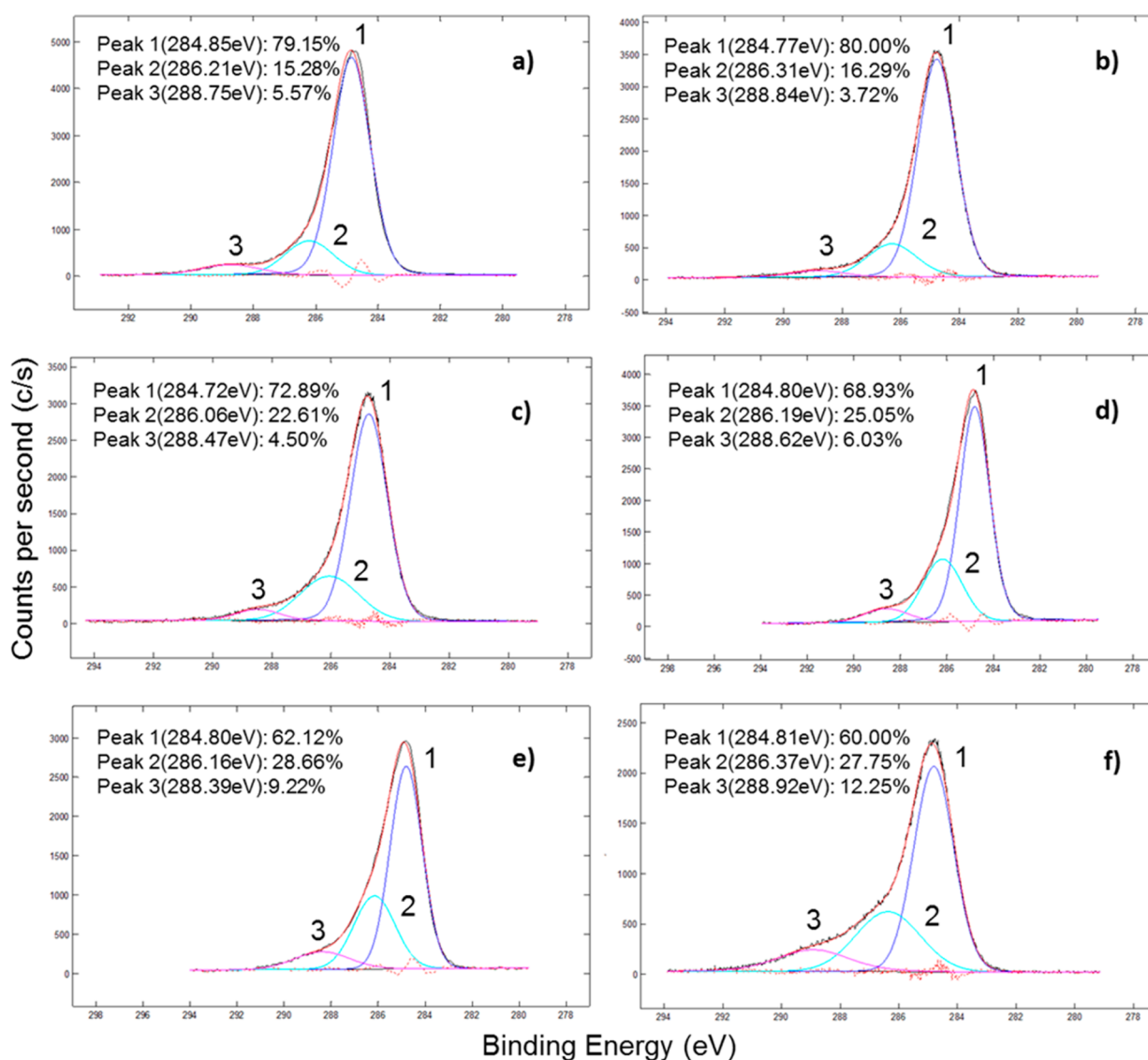
Figure 3. XPS data on nC60 for (a) aqueous sample and (b) aerosol sample without exposure, and for aerosol nC60 exposed at (c) 2.4, (d) 7.9, (e) 13.3, and (f) 17.2 equiv days of aging. Peaks 1−3 correspond to underivatized, mono-oxidized, and dioxidized carbon in that order.

Table 1. XPS Peak Fitted Data

OH exposure (molec. cm^{-3} s)	equivalent age (days)	underivatized carbon (% area)	mono-oxidized carbon (% area)	dioxidized carbon (% area)
	0	80.00	16.29	3.72
$(3.14 \pm 0.16) \times 10^{11}$	2.42 ± 0.12	72.89	22.61	4.50
$(1.02 \pm 0.01) \times 10^{12}$	7.87 ± 0.10	68.93	25.05	6.03
$(1.73 \pm 0.02) \times 10^{12}$	13.3 ± 0.10	62.12	28.66	9.22
$(2.24 \pm 0.03) \times 10^{12}$	17.2 ± 0.20	60.00	27.75	12.25

photoelectron spectroscopy (XPS), as shown in Figure 3 and summarized in Tables 1 and S1. The peak position for underivatized fullerene carbon in our samples lies between 284.72 and 284.85 eV, comparable to the value published by NIST of 285.10 eV[57] and observed elsewhere.[53,58] Over the mimicked age span of ∼17 days, the total amount of surface-based underivatized carbon decreases from 80.00% to 60.00%, mono-oxidized carbon (286.06−286.37 eV) increases from 16.29% to 27.75%, and dioxidized carbon (288.39−288.92 eV) increases from 3.72% to 12.25% (Figure 4). Peak positions for the mono and dioxidized carbon are similar to those published for bulk C_{60} ozonolysis[26] and soot ozonolysis,[59] however the

relative contributions to total oxygen content on the surface differs, suggesting a pathway controlled by other reactants (such as $^\bullet$OH). The trend of the data in Figure 4 does not plateau, suggesting surface saturation is not likely achieved throughout exposure, despite the considerable conversion of underivatized carbon.

In aqueous media, light sensitized reactions are believed to involve a chemical pathway (primarily through $^\bullet$OH) given considerable retardation in reaction kinetics when no oxygen is present.[19] While beyond the scope of this initial study, we do encourage future studies to consider specific oxidative reactants to delineate chemical pathways. For such delineation, UV
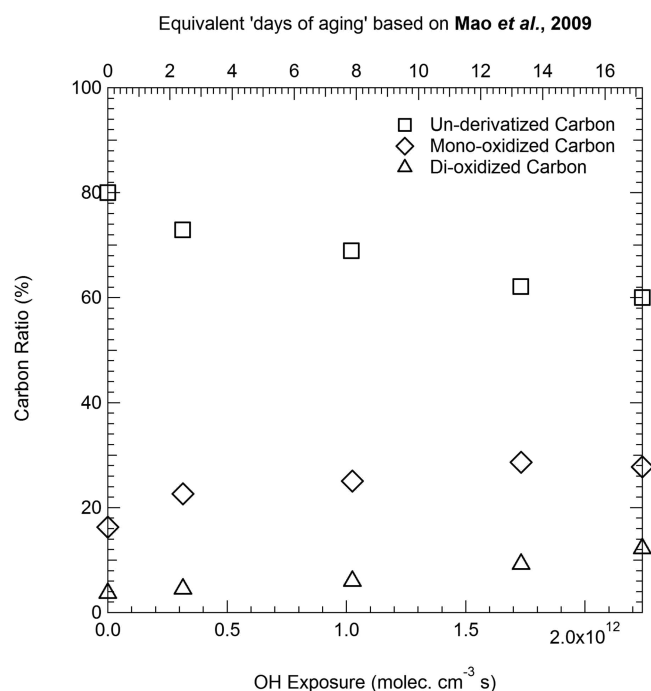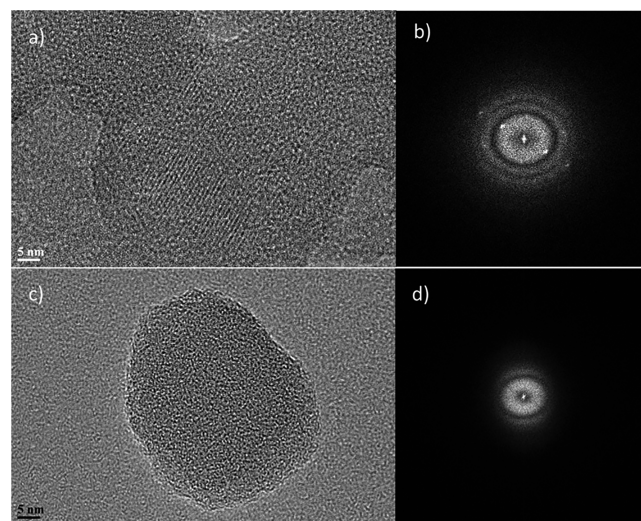
Figure 4. Integrated peak areas from XPS data as a function of OH Exposure for differently hybridized carbon.

microscopy (HR-TEM) images (Figure 5) and X-ray diffraction (XRD) patterns (Figure S4) were evaluated for parent and

Figure 5. Transmission electron microscopy data for unoxidized nC_{60} displayed as (a) HR-TEM image and (b) fast Fourier Transform (FFT) pattern, and oxidized nC_{60} (16.1 equiv days of aging) displayed as (c) HR-TEM image and (d) FFT pattern.

excitation should also be considered, as it has been observed to facilitate electron transfer from conjugated π systems to electron acceptors.[16] Additionally, the carbon−carbon double bonds found in nC_{60}, considering a nonconjugated system as a hypothetical resonance structure, are susceptible to radical attack under irradiation.[19,60] In water, it has been observed that nC_{60} once excited to a triplet state, can subsequently sensitize the formation of singlet oxygen ($^1O_2$).[19] In our system, this phenomenon may be enhanced for two reasons: the photolysis of ozone yields O(^{1}D) that can in turn excite ground state molecular oxygen, and the collision probability of ground-state oxygen with excited-state nC_{60} is likely higher due to higher gas-phase diffusivity of reactants vs aqueous-phase diffusivities. In both cases, oxygen can act as an electron withdrawing group, leaving the donating ring on nC_{60} susceptible to nucleophilic addition of the hydroxyl radical, forming OH-adducts.[60] Although the surface reaction may be faster than in the aqueous phase, the gas-phase environment does not allow dissolution (or "peeling") of the hydrophilic outer shell, lowering the observed (bulk) rate of reaction.

Loss of Crystallinity. Diffusion time scales for gaseous oxidants in a (solid) crystal structure of pristine nC_{60} can be expected to be on the scale of years (for a 100 nm aerosol and assuming a diffusion coefficient of oxidants in $nC_{60} > 10^{-19}$ cm^2 s^{-1}, typical for crystalline solids[61]), which is considerably longer than atmospheric reaction time scales. However, if aerosol-phase surface reaction morphs the pristine structure, the diffusion time scales can be significantly affected, and the observed rate of reaction would also change. For example, trace levels of hydrogen chloride (HCl) gas has been shown to induce disorder on ice surfaces in a temperature range of 186 to 243 K.[62] This explains why reported values for diffusion coefficients of HCl on ice vary dramatically on different ice surfaces.[63,64] If atmospheric photo-oxidants could have similar effects on nC_{60} surfaces, reaction rates would not be as slow as expected. To explore this, high resolution transmission electron

oxidized samples. Results suggest that crystallinity is lost upon oxidation; however, persistence of peaks at ca. 520 and 570 cm^{-1} (parent peaks) in FTIR spectra suggest that parent C_{60} does exist, to some degree in the aggregate (likely in the aerosol core). While this would challenge the suggestion that reaction (chemical or physical) is surface-limited, without further investigation, it is not straightforward to assess the underlying mechanism that drives the observed disorder. Underpinning this process, several phenomena may be responsible, including (i) increased surface disorder, either allowing oxidants to diffuse to the core more readily or (ii) rearrangement of product molecules to the core that, although involving an enthalpic penalty, are entropically preferred. Owing to the cage structure of a C_{60} molecule and its (caged) products, the enthalpic cost of breaking a $\pi−\pi$ stacking interactions is likely not strong enough to hinder disorder in the nanoparticle. Other possibilities include (iii) intercalated water within the nanoparticle aggregate, which upon UV light irradiation, releases ROS that readily react with the core, or unexpected ligand-induced rearrangements[65] or (iv) a purely UV-light sensitized rearrangement of the nanoparticle structure that, although interesting, is not relevant to tropospheric chemistry. We suggest excluding possibility (ii) due to the unlikeliness of entropic processes dominating enthalpic processes (over the explored reaction times) and (iii) due to FTIR data not showing dramatic decrease in the parent peaks upon oxidation. The only way possibility (iv) would be excluded is by assuming that work done by Lee et al.,[19] which implies that the free oxygen's role has a fundamental effect on crystal structure as well. OFRs like the PAM reactor operate on τ_{res} values on the order of seconds to minutes, which is short compared to an average aerosol lifetime in the troposphere. Therefore, we can not quantify the effect of diffusion on atmospheric photo-oxidation for nC_{60}. David et al. suggest that >260 K, C_{60} molecules undergo (continuous) reorientation;[66] therefore, although atmospheric photooxidation is not a high energy

process, it may be enough to destabilize $\pi-\pi$ stacking in the outer lattice and induce disorder in the crystal structure.

For reacted samples, XPS spectra are different from those observed for samples produced by the aqueous phase reaction of nC_{60} with ozone, as published by Fortner et al.[8] Ozonation of aqueous nC_{60} yields more dioxidized than mono-oxidized carbon (30% and 18%, respectively, from XPS fitted peak areas), whereas in this study, fullerenes subject to the highest $^{\bullet}OH$ exposure of $\sim2.24 \times 10^{12}$ molec. cm^{-3} s (~17.3 equiv days of aging) yielded comparatively more mono-oxidized than dioxidized carbon (27.8% and 12.3%, respectively, from XPS peak area), and the remaining underivatized carbon fraction was higher (52% for the aqueous study and 60.0% for this study). For these, resulting spectra are more similar to that of the aqueous phase reaction of nC_{60} with $^{\bullet}OH$ as described by Lee et al., although the mono-oxidized carbon fraction of the area is much higher for aqueous-phase oxidation (53.64% for the aqueous study and 27.8% for this study at ~17.3 equiv days of aging).

Environmental Implications. In this study, we observe direct evidence of atmospheric oxidation of C_{60}. However, in relatively dry conditions ($\sim30\%$ RH), even a very strong oxidizing atmosphere yields a relatively limited reaction of the material. Based on the decay of underivatized carbon via XPS analysis, we estimate the atmospheric photochemical lifetime of nC_{60} to be 1−2 months, meaning wet and dry deposition would remain the dominant atmospheric loss pathways. Such a slow oxidation mechanism helps explain detection of aerosol-bound fullerenes even in the Mediterranean basin,[25] far removed from anthropogenic sources. The reactive and effective uptake coefficients for nC_{60} to O_3 or $^{\bullet}OH$ has not been calculated due to coupling of the oxidants (hydroxylation photochemistry versus ozonolysis), as well as complex mixing patterns in the reactor, and while important, are beyond the scope of this work. It is worth mentioning that Pillar et al.[67] used an effective uptake coefficient of ozone on catechol at the air-water interface of 2.73×10^{-7} and an effective uptake of $\bullet OH$ between 0.01 and 1, to estimate a range of reaction rates for O_3 with catechol, which were 1 − 100 times that of $\bullet OH$ to catechol for mean tropospheric values. However, this is dependent on forming the initial ozonide, which when considering C_{60}'s caged structure, becomes less favorable. Given our estimate of nC_{60}'s photochemical lifetime is on the order of months, compared to hours for catechol from Pillar et al., we take caution in extending their values to our system. Taken together, with light sensitizing the reaction by both producing $^{\bullet}OH$ and promoting C_{60} to its excited triplet state, we believe both in the PAM and in the troposphere, that $^{\bullet}OH$ oxidation accounts for more nC_{60} depletion than O_3 oxidation. We do however recognize that in the PAM this reaction could be augmented artificially because of the UV light required in $^{\bullet}OH$ generation.

Of interest in future work is to understand interactions with fogwater or cloudwater (e.g., how uptake kinetics vary as a function of dry aerosol age) using both dry aerosolization techniques (e.g., Tiwari et al.)[27] and wet aerosolization techniques (this work). Functionalizing the surface should increase the hydrophilicity of the nanoparticle, however if, once scavenged, the outer layer sheds (is solubilized) into solution, the freshly exposed hydrophobic surface may repartition to the aerosol phase, where it can undergo further aerosol phase oxidation. This could be important for reactions in deliquesced aerosols, as discussed. Cloud seeding, where an increase in

polarity on the surface of the nanoparticles may cause them to act as more efficient cloud condensation nuclei (CCN), can become important at tropical latitudes where clouds are warmer, but not as effective at higher latitudes or altitudes where ice nuclei (IN) become more important. Furthermore, wildfires and agricultural activity at those latitudes result in a consistent source of soot aerosols, likely containing fullerenes and/or fullerene-like materials. Increased light exposure yields consistent vertical profiles of $^{\bullet}OH$,[46] which can become a dominant oxidant at higher altitudes, thus increasing the potential for hydroxy-based photochemistries to play a significant role in fullerene reactivity in the free troposphere.

■ ASSOCIATED CONTENT

ⓢ Supporting Information

The Supporting Information is available free of charge on the ACS Publications website at DOI: 10.1021/acsearthspace-chem.7b00116.

SI includes: nC_{60} nanocrystal synthesis, setup details, detailed explanation of Figure 1, schematic of the setup to study aerosol-phase oxidation, size distributions of nanoparticles in the aqueous phase compared to the aerosol phase, in-house calibration of the potential aerosol mass reactor, X-ray diffraction spectra, and complete set of recorded values (PDF)

■ AUTHOR INFORMATION

Corresponding Authors

*Address: One Brookings Drive, Brauer 1015, St. Louis, Missouri, 63130. E-mail (J.D.F.): jfortner@wustl.edu. Telephone: (314) 935-9293.

*Address: One Brookings Drive, Brauer 3026, St. Louis, Missouri, 63130. E-mail (B.J.W.): brentw@wustl.edu. Telephone: (314) 935-9279.

ORCID ⓘ

Dhruv Mitroo: 0000-0002-7398-2020

Michael J. Walker: 0000-0003-1347-7636

Present Address

‡Dhruv Mitroo: Rosenstiel School of Marine and Atmospheric Sciences, University of Miami, Miami, Florida 33149, USA.

Notes

The authors declare no competing financial interest.

■ REFERENCES

(1) Nowack, B. The behavior and effects of nanoparticles in the environment. *Environ. Pollut.* **2009**, *157* (4), 1063−1064.

(2) Biswas, P.; Wu, C.-Y. Nanoparticles and the Environment. *J. Air Waste Manage. Assoc.* **2005**, *55* (6), 708−746.

(3) Wong, S.; Karn, B. Ensuring sustainability with green nano-technology. *Nanotechnology* **2012**, *23* (29), 290201−290201.

(4) Bakry, R.; Vallant, R. M.; Najam-ul-Haq, M.; Rainer, M.; Szabo, Z.; Huck, C. W.; Bonn, G. K. Medicinal applications of fullerenes. *Int. J. Nanomedicine* **2007**, *2* (4), 639−649.

(5) Tremblay, J.-F. Mitsubishi Chemical Aims at Breakthrough. *Chem. Eng. News* **2002**, *80* (49), 16−17.

(6) Buseck, P. R.; Adachi, K. Nanoparticles in the Atmosphere. *Elements* **2008**, *4* (6), 389−394.

(7) Nowack, B.; Bucheli, T. Occurrence, behavior and effects of nanoparticles in the environment. *Environ. Pollut.* **2007**, *150* (1), 5−22.

(8) Fortner, J. D.; Kim, D.-I.; Boyd, A. M.; Falkner, J. C.; Moran, S.; Colvin, V. L.; Hughes, J. B.; Kim, J.-H. Reaction of Water-Stable C_{60} Aggregates with Ozone. *Environ. Sci. Technol.* **2007**, *41* (21), 7497−7502.

(9) Li, Y.; Niu, J.; Shang, E.; Crittenden, J. C. Synergistic Photogeneration of Reactive Oxygen Species by Dissolved Organic Matter and C_{60} in Aqueous Phase. *Environ. Sci. Technol.* **2015**, *49* (2), 965−973.

(10) Sayes, C. M.; Fortner, J. D.; Guo, W.; Lyon, D.; Boyd, A. M.; Ausman, K. D.; Tao, Y. J.; Sitharaman, B.; Wilson, L. J.; Hughes, J. B.; et al. The Differential Cytotoxity of Water-Soluble Fullerenes. *Nano Lett.* **2004**, *4* (10), 1881−1887.

(11) Howard, J. B.; McKinnon, J. T.; Makarovsky, Y.; Lafleur, A. L.; Johnson, M. E. Fullerenes C60 and C70 in flames. *Nature* **1991**, *352* (6331), 139−141.

(12) Heymann, D. Search for C_{60} Fullerene in Char Produced on a Norway Spruce by Lightning. *Fullerene Sci. Technol.* **1998**, *6* (6), 1079−1086.

(13) Benn, T.; Herckes, P.; Westerhoff, P. Fullerenes in Environmental Samples: C_{60} in Atmospheric Particulate Matter. In *Comprehensive Analytical Chemistry*; Elsevier, 2012; Vol. 59, pp 291−303.

(14) Lee, J.; Song, W.; Jang, S. S.; Fortner, J. D.; Alvarez, P. J. J.; Cooper, W. J.; Kim, J.-H. Stability of Water-Stable C_{60} Clusters to OH Radical Oxidation and Hydrated Electron Reduction. *Environ. Sci. Technol.* **2010**, *44* (10), 3786−3792.

(15) Wu, J.; Benoit, D.; Lee, S. S.; Li, W.; Fortner, J. D. Ground State Reactions of nC_{60} with Free Chlorine in Water. *Environ. Sci. Technol.* **2016**, *50* (2), 721−731.

(16) Hirsch, A.; Brettreich, M. *Fullerenes: Chemistry and Reactions*; Wiley-VCH Verlag GmbH & Co. KGaA: Weinheim, Germany, 2004.

(17) Heymann, D.; Bachilo, S. M.; Weisman, R. B.; Cataldo, F.; Fokkens, R. H.; Nibbering, N. M. M.; Vis, R. D.; Chibante, L. P. F. $C_{60}O_3$, a Fullerene Ozonide: Synthesis and Dissociation to $C_{60}O$ and O_2. *J. Am. Chem. Soc.* **2000**, *122* (46), 11473−11479.

(18) Malhotra, R.; Kumar, S.; Satyam, A. Ozonolysis of [60]fullerene. *J. Chem. Soc., Chem. Commun.* **1994**, No. 11, 1339.

(19) Lee, J.; Cho, M.; Fortner, J. D.; Hughes, J. B.; Kim, J.-H. Transformation of Aggregated C_{60} in the Aqueous Phase by UV Irradiation. *Environ. Sci. Technol.* **2009**, *43* (13), 4878−4883.

(20) Arbogast, J. W.; Darmanyan, A. P.; Foote, C. S.; Diederich, F. N.; Whetten, R. L.; Rubin, Y.; Alvarez, M. M.; Anz, S. J. Photophysical properties of sixty atom carbon molecule (C60). *J. Phys. Chem.* **1991**, *95* (1), 11−12.

(21) Krusic, P. J.; Wasserman, E.; Parkinson, B. A.; Malone, B.; Holler, E. R.; Keizer, P. N.; Morton, J. R.; Preston, K. F. Electron spin resonance study of the radical reactivity of C60. *J. Am. Chem. Soc.* **1991**, *113* (16), 6274−6275.

(22) Yamakoshi, Y.; Umezawa, N.; Ryu, A.; Arakane, K.; Miyata, N.; Goda, Y.; Masumizu, T.; Nagano, T. Active Oxygen Species Generated from Photoexcited Fullerene (C_{60}) as Potential Medicines: $O_2^{-\bullet}$ versus $^1O_2$. *J. Am. Chem. Soc.* **2003**, *125* (42), 12803−12809.

(23) Lee, J.; Yamakoshi, Y.; Hughes, J. B.; Kim, J.-H. Mechanism of C_{60} Photoreactivity in Water: Fate of Triplet State and Radical Anion and Production of Reactive Oxygen Species. *Environ. Sci. Technol.* **2008**, *42* (9), 3459−3464.

(24) Utsunomiya, S.; Jensen, K. A.; Keeler, G. J.; Ewing, R. C. Uraninite and Fullerene in Atmospheric Particulates. *Environ. Sci. Technol.* **2002**, *36* (23), 4943−4947.

(25) Sanchís, J.; Berrojalbiz, N.; Caballero, G.; Dachs, J.; Farré, M.; Barceló, D. Occurrence of Aerosol-Bound Fullerenes in the Mediterranean Sea Atmosphere. *Environ. Sci. Technol.* **2012**, *46* (3), 1335−1343.

(26) Tiwari, A. J.; Morris, J. R.; Vejerano, E. P.; Hochella, M. F.; Marr, L. C. Oxidation of C_{60} Aerosols by Atmospherically Relevant Levels of O_3. *Environ. Sci. Technol.* **2014**, *48* (5), 2706−2714.

(27) Liu, Y.; Liggio, J.; Li, S.-M.; Breznan, D.; Vincent, R.; Thomson, E. M.; Kumarathasan, P.; Das, D.; Abbatt, J.; Antiñolo, M.; et al. Chemical and Toxicological Evolution of Carbon Nanotubes During Atmospherically Relevant Aging Processes. *Environ. Sci. Technol.* **2015**, *49*, 2806−2814.

(28) Wang, J.; Onasch, T. B.; Ge, X.; Collier, S.; Zhang, Q; Sun, Y.; Yu, H.; Chen, M.; Prevót, A. S. H.; Worsnop, D. R. *Environ. Sci. Technol. Lett.* **2016**, *3*, 121−126.

(29) Farré, M.; Barceló, D.; Farré, M. *Analysis and risk of Nanomaterials in Environmental and Food Samples*, 1st ed.; Comprehensive Analytical Chemistry; Elsevier: Amsterdam, 2012.

(30) Katrib, Y.; Biskos, G.; Buseck, P. R.; Davidovits, P.; Jayne, J. T.; Mochida, M.; Wise, M. E.; Worsnop, D. R.; Martin, S. T. Ozonolysis of Mixed Oleic-Acid/Stearic-Acid Particles: Reaction Kinetics and Chemical Morphology. *J. Phys. Chem. A* **2005**, *109* (48), 10910−10919.

(31) Smith, J. D.; Kroll, J. H.; Cappa, C. D.; Che, D. L.; Liu, C. L.; Ahmed, M.; Leone, S. R.; Worsnop, D. R.; Wilson, K. R. The heterogeneous reaction of hydroxyl radicals with sub-micron squalane particles: a model system for understanding the oxidative aging of ambient aerosols. *Atmos. Chem. Phys.* **2009**, *9* (9), 3209−3222.

(32) McNeill, V. F.; Yatavelli, R. L. N.; Thornton, J. A.; Stipe, C. B.; Landgrebe, O. Heterogeneous OH oxidation of palmitic acid in single component and internally mixed aerosol particles: vaporization and the role of particle phase. *Atmos. Chem. Phys.* **2008**, *8* (17), 5465−5476.

(33) Kessler, S. H.; Smith, J. D.; Che, D. L.; Worsnop, D. R.; Wilson, K. R.; Kroll, J. H. Chemical Sinks of Organic Aerosol: Kinetics and Products of the Heterogeneous Oxidation of Erythritol and Levoglucosan. *Environ. Sci. Technol.* **2010**, *44* (18), 7005−7010.

(34) Kwamena, N.-O. A.; Staikova, M. G.; Donaldson, D. J.; George, I. J.; Abbatt, J. P. D. Role of the Aerosol Substrate in the Heterogeneous Ozonation Reactions of Surface-Bound PAHs. *J. Phys. Chem. A* **2007**, *111* (43), 11050−11058.

(35) Kwamena, N.-O. A.; Thornton, J. A.; Abbatt, J. P. D. Kinetics of Surface-Bound Benzo[*a*]pyrene and Ozone on Solid Organic and Salt Aerosols. *J. Phys. Chem. A* **2004**, *108* (52), 11626−11634.

(36) Bedjanian, Y.; Nguyen, M. L. Kinetics of the reactions of soot surface-bound polycyclic aromatic hydrocarbons with O3. *Chemosphere* **2010**, *79* (4), 387−393.

(37) Kang, E.; Root, M. J.; Toohey, D. W.; Brune, W. H. Introducing the concept of Potential Aerosol Mass (PAM). *Atmos. Chem. Phys.* **2007**, *7* (22), 5727−5744.

(38) Deguchi, S.; Alargova, R. G.; Tsujii, K. Stable Dispersions of Fullerenes, C_{60} and C_{70}, in Water. Preparation and Characterization. *Langmuir* **2001**, *17* (19), 6013−6017.

(39) Kang, E.; Toohey, D. W.; Brune, W. H. Dependence of SOA oxidation on organic aerosol mass concentration and OH exposure: experimental PAM chamber studies. *Atmos. Chem. Phys.* **2011**, *11* (4), 1837−1852.

(40) Lambe, A. T.; Onasch, T. B.; Massoli, P.; Croasdale, D. R.; Wright, J. P.; Ahern, A. T.; Williams, L. R.; Worsnop, D. R.; Brune, W. H.; Davidovits, P. Laboratory studies of the chemical composition and cloud condensation nuclei (CCN) activity of secondary organic aerosol (SOA) and oxidized primary organic aerosol (OPOA). *Atmos. Chem. Phys. Discuss.* **2011**, *11* (5), 13617−13653.

(41) Ortega, A. M.; Day, D. A.; Cubison, M. J.; Brune, W. H.; Bon, D.; de Gouw, J. A.; Jimenez, J. L. Secondary organic aerosol formation and primary organic aerosol oxidation from biomass-burning smoke in a flow reactor during FLAME-3. *Atmos. Chem. Phys.* **2013**, *13* (22), 11551−11571.

(42) Li, R.; Palm, B. B.; Ortega, A. M.; Hlywiak, J.; Hu, W.; Peng, Z.; Day, D. A.; Knote, C.; Brune, W. H.; de Gouw, J. A.; et al. Modeling the Radical Chemistry in an Oxidation Flow Reactor: Radical Formation and Recycling, Sensitivities, and the OH Exposure Estimation Equation. *J. Phys. Chem. A* **2015**, *119* (19), 4418−4432.

(43) Peng, Z.; Day, D. A.; Stark, H.; Li, R.; Lee-Taylor, J.; Palm, B. B.; Brune, W. H.; Jimenez, J. L. HOx radical chemistry in oxidation flow reactors with low-pressure mercury lamps systematically examined by modeling. *Atmos. Meas. Tech.* **2015**, *8* (11), 4863−4890.

(44) Lambe, A. T.; Ahern, A. T.; Williams, L. R.; Slowik, J. G.; Wong, J. P. S.; Abbatt, J. P. D.; Brune, W. H.; Ng, N. L.; Wright, J. P.; Croasdale, D. R.; et al. Characterization of aerosol photooxidation flow reactors: heterogeneous oxidation, secondary organic aerosol formation and cloud condensation nuclei activity measurements. *Atmos. Meas. Tech.* **2011**, *4* (3), 445−461.

(45) Renbaum, L. H.; Smith, G. D. Artifacts in measuring aerosol uptake kinetics: the roles of time, concentration and adsorption. *Atmos. Chem. Phys.* **2011**, *11* (14), 6881−6893.

(46) Mao, J.; Ren, X.; Brune, W. H.; Olson, J. R.; Crawford, J. H.; Fried, A.; Huey, L. G.; Cohen, R. C.; Heikes, B.; Singh, H. B.; et al. Airborne measurement of OH reactivity during INTEX-B. *Atmos. Chem. Phys.* **2009**, *9* (1), 163−173.

(47) Seinfeld, J. H. *Atmospheric Chemistry and Physics: From Air Pollution to Climate Change*, 2nd ed.; J. Wiley: Hoboken, NJ, 2006.

(48) Wang, L.; Wu, R.; Xu, C. Atmospheric Oxidation Mechanism of Benzene. Fates of Alkoxy Radical Intermediates and Revised Mechanism. *J. Phys. Chem. A* **2013**, *117* (51), 14163−14168.

(49) Zhang, Z.; Lin, L.; Wang, L. Atmospheric oxidation mechanism of naphthalene initiated by OH radical. A theoretical study. *Phys. Chem. Chem. Phys.* **2012**, *14* (8), 2645.

(50) Wu, R.; Pan, S.; Li, Y.; Wang, L. Atmospheric Oxidation Mechanism of Toluene. *J. Phys. Chem. A* **2014**, *118* (25), 4533−4547.

(51) Brant, J. A.; Labille, J.; Robichaud, C. O.; Wiesner, M. Fullerol cluster formation in aqueous solutions: Implications for environmental release. *J. Colloid Interface Sci.* **2007**, *314* (1), 281−288.

(52) Wu, J.; Alemany, L. B.; Li, W.; Petrie, L.; Welker, C.; Fortner, J. D. Reduction of Hydroxylated Fullerene (Fullerol) in Water by Zinc: Reaction and Hemiketal Product Characterization. *Environ. Sci. Technol.* **2014**, *48* (13), 7384−7392.

(53) Wu, J.; Goodwin, D. G.; Peter, K.; Benoit, D.; Li, W.; Fairbrother, D. H.; Fortner, J. D. Photo-Oxidation of Hydrogenated Fullerene (Fullerane) in Water. *Environ. Sci. Technol. Lett.* **2014**, *1* (12), 490−494.

(54) Scrivens, W. A.; Tour, J. M.; Creek, K. E.; Pirisi, L. Synthesis of 14C-Labeled C60, Its Suspension in Water, and Its Uptake by Human Keratinocytes. *J. Am. Chem. Soc.* **1994**, *116* (10), 4517−4518.

(55) Wei, X.; Wu, M.; Qi, L.; Xu, Z. Selective solution-phase generation and oxidation reaction of C60n− (n = 1,2) and formation of an aqueous colloidal solution of C60. *J. Chem. Soc., Perkin Trans. 2* **1997**, No. 7, 1389−1394.

(56) Alargova, R. G.; Deguchi, S.; Tsujii, K. Stable Colloidal Dispersions of Fullerenes in Polar Organic Solvents. *J. Am. Chem. Soc.* **2001**, *123* (43), 10460−10467.

(57) Werner, H.; Wesemann, M.; Schlögl, R. Electronic Structure of C$_{60}$ (I$_2$)$_{1.88}$: a Photoemission Study. *Europhys. Lett. EPL* **1992**, *20* (2), 107−110.

(58) Hou, W.-C.; Kong, L.; Wepasnick, K. A.; Zepp, R. G.; Fairbrother, D. H.; Jafvert, C. T. Photochemistry of Aqueous C$_{60}$ Clusters: Wavelength Dependency and Product Characterization. *Environ. Sci. Technol.* **2010**, *44* (21), 8121−8127.

(59) Orrling, D.; Fitzgerald, E.; Ivanov, A.; Molina, M. Enhanced sulfate formation on ozone-exposed soot. *J. Aerosol Sci.* **2011**, *42* (9), 615−620.

(60) Krusic, P. J.; Wasserman, E.; Keizer, P. N.; Morton, J. R.; Preston, K. F. Radical Reactions of C60. *Science* **1991**, *254* (5035), 1183−1185.

(61) Shiraiwa, M.; Ammann, M.; Koop, T.; Poschl, U. Gas uptake and chemical aging of semisolid organic aerosol particles. *Proc. Natl. Acad. Sci. U. S. A.* **2011**, *108* (27), 11003−11008.

(62) McNeill, V. F.; Loerting, T.; Geiger, F. M.; Trout, B. L.; Molina, M. J. Hydrogen chloride-induced surface disordering on ice. *Proc. Natl. Acad. Sci. U. S. A.* **2006**, *103* (25), 9422−9427.

(63) Huthwelker, T.; Ammann, M.; Peter, T. The Uptake of Acidic Gases on Ice. *Chem. Rev.* **2006**, *106* (4), 1375−1444.

(64) Flückiger, B.; Chaix, L.; Rossi, M. J. Properties of the HCl/Ice, HBr/Ice, and H$_2$O/Ice Interface at Stratospheric Temperatures (200 K) and Its Importance for Atmospheric Heterogeneous Reactions. *J. Phys. Chem. A* **2003**, *107* (15), 2768−2768.

(65) Klajn, R.; Bishop, K. J. M.; Grzybowski, B. A. Light-controlled self-assembly of reversible and irreversible nanoparticle suprastructures. *Proc. Natl. Acad. Sci. U. S. A.* **2007**, *104* (25), 10305−10309.

(66) David, W. I. F.; Ibberson, R. M.; Dennis, T. J. S.; Hare, J. P.; Prassides, K. Structural Phase Transitions in the Fullerene C60. *Europhys. Lett. EPL* **1992**, *18* (8), 735−736.

(67) Pillar, E. A.; Camm, R. C.; Guzman, M. I. Catechol Oxidation by Ozone and Hydroxyl Radicals at the Air−Water Interface. *Environ. Sci. Technol.* **2014**, *48* (24), 14352−14360.